Su(var)3-9 mediates age-dependent increase in H3K9 methylation on TDP-43 promoter triggering neurodegeneration

Marta Marzullo[#1,2], Giulia Romano[#3], Claudia Pellacani[1,2], Federico Riccardi[3], Laura Ciapponi[2]* and Fabian Feiguin[4]*

[1]Istituto di Biologia e Patologia Molecolari del CNR, Sapienza Università di Roma, Roma, Italy.

[2]Dipartimento di Biologia e Biotecnologie "C. Darwin", Sapienza Università di Roma, Roma, Italy.

[3]International Centre for Genetic Engineering and Biotechnology, Padriciano 99, 34149 Trieste, Italy.

[4]Department of Life and Environmental Sciences, University of Cagliari, 09042 Monserrato, Cagliari, Italy.

[#] Equally contributing authors

[*] Corresponding authors

E-mail: laura.ciapponi@uniroma1.it or fabian.feiguin@unica.it

Abstract

Aging progressively modifies the physiological balance of the organism increasing susceptibility to both genetic and sporadic neurodegenerative diseases. These changes include epigenetic chromatin remodeling events that may modify gene transcription. However, how aging interconnects with disease-causing genes is not well known. Here, we found that Su(var)3-9 causes increased methylation of histone H3K9 in the promoter region of TDP-43, the most frequently altered factor in amyotrophic lateral sclerosis (ALS), affecting the mRNA and protein expression levels of this gene through epigenetic modifications in chromatin organization that appear to be conserved in aged *Drosophila* brains, mouse and human cells. Remarkably, augmented Su(var)3-9 activity causes a decrease in TDP-43 expression followed by early defects in locomotor activities. In contrast, decreasing Su(var)3-9 action promotes higher levels of TDP-43 expression and reinvigorates motility parameters in old flies, uncovering a novel role of this enzyme in regulating TDP-43 expression and locomotor senescence. The data indicate how conserved epigenetic mechanisms may link aging with neuronal diseases and suggest that Su(var)3-9 may play a role in the pathogenesis of ALS.

Introduction

Aging is associated with a series of molecular changes, that lead to functional tissue deterioration and predispose to an increased likelihood of disease and death. This process, interestingly, does not seem to happen randomly, but follows a programmed sequence of events that appear to be conserved among evolutionarily divergent species (1–3). In the nervous system, neuronal aging or senescence can be functionally quantified through two main phenotypes, the deterioration of cognitive functions and the reduction of locomotory capacities. These alterations, on the other hand, coincide with the insidious symptoms that signal the onset and progression of the most common neurodegenerative diseases such as Alzheimer's disease (AD), Parkinson's disease (PD) or amyotrophic lateral sclerosis (ALS) (4,5) endorsing the idea that aging and pathological neurodegeneration may be regulated by a common set of genes (6,7).

Molecularly, a common feature of aging is the epigenetic changes in chromatin organization that occur after the post-translational modifications of histones (8,9). These modifications are conserved, affect the expression parameters of numerous genes, and may provoke alterations in the expression levels of proteins that constitute risk factors for neurodegenerative diseases. In support of this view, we and others have described that defects in the conserved TDP-43 (encoded by the *TARDBP* gene), a member of the heterogeneous nuclear ribonucleoproteins (hnRNPs) family and largely associated with the pathogenesis of ALS (10–12), is permanently required in the nervous system to maintain locomotor activity and becomes downregulated during aging in *Drosophila* and mammalian brains (13–16). Moreover, TDP-43 tight regulation in humans is required also in other tissues (such as glia and skeletal muscles) to maintain the correct molecular organization of the neuromuscular synapses and muscular innervation, all aspects critical for the motor system functioning (17–21). Even though these fluctuations in protein levels appear to be consistent and conserved in highly

different species, the physiological relevance of reduced TDP-43 expression during aging, the molecules involved, and their contribution to neuronal senescence is not known. In this study, we investigated the mechanisms by which TDP-43 becomes downregulated during aging and the functional implications of these modifications in the onset and progression of locomotor waning.

Results

Recovery of TDP-43 function during aging prevents locomotor decline

Progressive degeneration in locomotor activity, also known as locomotor senescence, is one of the main phenotypes used to quantify the impact of age on the functional organization of the nervous system and negative geotaxis (the ability of flies to vertically climb a test cylinder) a well-accepted assay for measuring neuromuscular capacity *in vivo* (22,23). Using this methodology, we have described that the progressive decrease in *Drosophila* locomotor activity during aging correlates with a physiological decrease in the expression of the TBPH protein, homologous to the human TDP-43 (15). Consistently, we and others showed that also in mice TDP-43 undergoes an aging-dependent decrease (15,16), highlighting the evolutionary relevance of this phenomenon. However, the relationships between these events have not been clarified yet. To determine whether the drop in TBPH/TDP-43 expression during aging plays any role in locomotor senescence, we used the GeneSwitch (GS) system to generate flies carrying the neuronal driver *elav*-GS-GAL4 and the transgene UAS-TBPH (w^{1118}; UAS-TBPH/+; *elav*-GS-GAL4/+) to modulate the expression of TBPH in a temporally controlled manner by adding the RU-486 (mifepristone) activator in the fly food (14,24,25). As controls, we utilized the $TBPH^{F/L}$ allele unable to bind the RNA (w^{1118}; UAS-$TBPH^{F/L}$/+; *elav*-GS-GAL4/+) and the unrelated protein GFP (w^{1118}; UAS-EGFP/+; *elav*-GS-GAL4/+) (26). Thus, we detected that GS-flies in which the promoter was not activated,

showed a significant decrease in locomotor activity around 7 days post eclosion (dpe). This diminution in fly motility increases progressively during aging (50% at 14 dpe to 30% of their initial capacity at 21 dpe) and correlates with a decrease in TBPH/TDP-43 mRNA and protein levels (Supplementary Figure S1). Thus, to determine whether TBPH reintroduction in aged animals may prevent locomotor senescence, we induced the expression of the UAS-TBPH transgene (w^{1118}; UAS-TBPH/+; *elav*-GS-GAL4/+) in 18 days old flies during 72 hours, by adding the RU486 activator to the fly food (Figure 1A-B). Notably, we found that induction of TBPH expression improved climbing abilities and slowed the locomotor decline in aged flies compared to UAS-$TBPH^{F/L}$ (Figure 1C), establishing a direct correlation between the age-related decrease in TBPH expression and locomotor deterioration.

H3K9 methylation at the *TARDBP*/*TBPH* promoter increases with aging and is conserved in both flies and mammals

Gene expression is a tightly regulated process influenced by the epigenetic modifications of the histones, that control the accessibility to the DNA (in particular those located in promoter regions) to a large number of proteins that can directly promote the regulation of transcription (27,28). Mechanistically, the methylation of the histone H3K9 (H3K9me) by specific methyltransferase enzymes, constitutes the initial event that triggers the formation of repressive heterochromatin domains in the DNA (29,30). Thus, to determine if the downregulation of *TBPH* during *Drosophila* aging is related to changes in the methylation patterns of H3K9, we performed chromatin immunoprecipitation (ChIP) studies and assessed the binding profile of H3K9me3 on the *TBPH* promoter. Remarkably, we found a significant enrichment in H3K9me3 amounts sited on the *TBPH* promoter in chromatin samples extracted from old flies compared to young controls (Figure 2A), revealing an increase in the levels of repressive heterochromatin modifications on the *TBPH* promoter *in vivo* during

aging (16,30,31). In support of this observation, we noted that these epigenetic changes do not appear to be due to a generalized and/or nonspecific increase in H3K9 methylation caused by age, as its overall biochemical levels appear to decrease in old brains (Supplementary Figure S2), suggesting that the modifications described on the *TBPH* promoter are rather specific and may promote transcriptional repression of this gene. Importantly, we observed that similar modifications in H3K9 methylation levels of the TDP-43 promoter, take place also in the mammalian brain. Thus, H3K9me3 chromatin immunoprecipitation assays in C57 mice brains at post-natal day 10 (PND 10) and PND 365, showed a very significant increase (~20 fold) in the methylation levels of the *TARDBP* promoter in old mice compared to young samples or to unrelated controls (Figure 2B), revealing that these modifications follow well-conserved designs.

Su(var)3-9 mediated H3K9 methylation of the _TBPH_ promoter regulates gene expression levels and locomotor aging in flies

In order to explore the physiological significance of increased H3K9 methylation in the *TBPH* promoter region, we decided to modulate the activity of Su(var)3-9, the well-described and conserved histone methyltransferases capable of methylating H3K9 *in vivo* (30,32). Strikingly, we found that null alleles of *Su(var)3-9*, in trans-heterozygous combinations (*Su(var)3-9*^{6}*/ Su(var3-9*^{1}), sired viable and fertile flies that present a significant increase in their locomotor capacities in adulthood compared to age-matched controls in climbing assays (Figure 3A; Supplementary video V1). Accordingly, the locomotor performance of either 20, 30, or 40 days old *Su(var)3-9* mutant flies significantly exceeded the climbing abilities of wildtype flies of the same age. Along these lines, we quantified that the loss of locomotor capacity in *Su(var)3-9* mutant flies between 3 and 30 days after hatching (from 84% of flies reaching the top to 66%, respectively) was much less pronounced than in wildtype controls

(from 83% to 12%, respectively), underlining the unexpected role of this enzyme in regulating locomotor performances and neurological senescence (Figure 3A). Furthermore, biochemical analyses performed on fly head extracts obtained from the flies described above (3 and 20 days-old trans-heterozygous combinations *Su(var)3-9*^{6}*/Su(var)3-9*^{1} or *w*^{1118} wildtype controls), revealed that both *TBPH* mRNA and protein levels are higher in *Su(var)3-9* mutants compared to the wildtype controls (Figure 3B-C). Moreover, ChIP analyses, showed that *Su(var)3-9* old mutant flies presented reduced levels of H3K9 methylation in the promoter and coding regions of *TBPH* compared to controls (Figure 3D), indicating that these molecular differences in methylation and expression levels may underlie the phenotypic changes in motility. In support of this hypothesis, we found that overexpression of *UAS-Su(var)3-9* or its human counterpart *UAS-SUV39H1*, under the control of the neuronal driver *elav*-GAL4 (Supplementary Figure S3A), was sufficient to deeply affect the locomotor capacities of these flies, inducing early locomotor decline and provoking a strong reduction in the levels of TBPH protein expression in *Drosophila* brains (Figure 3E-F), revealing that Su(var)3-9 plays a major role in the epigenetic control of TBPH expression. Additionally, we found that incubation of wildtype *Drosophila* brains with chaetocin (unfortunately the compound, in the present formulation, does not pass the gastric barrier to be tested *in vivo*) causes an increase in *TBPH* expression and a reduction in H3K9 methylation, mimicking the effect caused by the loss of *Su(var)3-9* (Supplementary Figure S3B). Remarkably, we observed that the role of Su(var)3-9 in the regulations of *TBPH* promoter was rather specific since the loss of two additional enzymes able to methylate H3K9, like eggless and G9a in *Drosophila* (30), was unable to modify the expression levels of TBPH in fly heads or affect locomotor behaviors *in vivo* (Supplementary Figure S3C-E). Curiously, we observed that the expression of the *Drosophila* homolog of Fus (dFUS-*cabeza*), a gene epistatically related to

TBPH and ALS-related factor (12,33), does not change over time (Supplementary Figure S3F), suggesting that the age-dependent decline is specifically related to *TBPH* transcription.

The conserved SUV39H1 enzyme regulates TDP-43 expression levels in human cells

To determine if the conserved SUV39H1 histone methyltransferase is able to regulate the methylation of the TDP-43 promoter and modulate protein expression also in human cells, we took advantage of a HaCaT cell line carrying a CRISPR-Cas9 mutation in the *SUV39H1* gene (*SUV39H1 KO*; (34). Interestingly, we observed that in these cells the absence of SUV39H1 causes an increase in the levels of TDP-43 protein expression (Figure 4A). In the same direction, H3K9me3 ChIP analyses revealed a significant reduction in H3K9me3 amounts sited on the *TARDBP* promoter in chromatin samples extracted from SUV39H1 KO cells compared to wildtype cells (Figure 4B), suggesting that epigenetic modifications mediated by SUV39H1 might be responsible for the transcriptional repression of *TARDBP* and, above all, underlining the remarkable conservation found in the regulation of this locus. To challenge whether aging-induced modifications would also play a role in the regulation of human TDP-43, we treated wildtype or SUV39H1 KO cells with H_2O_2 a classic and well-accepted treatment for inducing cellular senescence (35–37); (Supplementary Figure S4). As a result, we found that H_2O_2 induced a significant reduction in TDP-43 protein expression which is prevented by the deletion of the *SUV39H1* gene (Figure 4C), indicating that similar age-dependent regulatory mechanisms might be present in human cells.

Discussion

One of the most fundamental features of aging is the progressive deterioration in locomotor skills. Despite some studies, in both mice and flies revealing that TDP-43/TBPH levels decrease during aging (15,16,38), the mechanism underlying aging-dependent locomotor

senescence and the accompanying physiological decrease of TDP-43 is unclear. Likewise, it is not obvious whether the lowering of TDP-43 levels leads to a locomotor decline in the elderly. In this manuscript, we found that induction of the TDP-43 fly counterpart, TBPH, expression in old fly neurons, but not of the $TBPH^{F/L}$ mutated form (unable to bind RNA), is sufficient to rescue locomotor senescence, demonstrating a direct correlation between these events and revealing a novel role for TDP-43/TBPH in the regulation of age-dependent locomotor degeneration. In that direction, alteration in the function of TDP-43 is considered one of the main causes of ALS and it has been shown that pathological variations in the intracellular levels of this protein (both gain or loss of function) were able to cause neuronal death indicating that tight control of TDP-43 expression is crucial to prevent neurological phenotypes (39–41). These observations, therefore, highlight the importance that the knowledge of novel genes or molecules capable to modulate TDP-43 activity could have for understanding the pathogenesis of ALS (42–45). According to that, we found an age-dependent increase in H3K9 methylation at the TBPH/TDP-43 promoter region mediated by *Su(var)3-9* in *Drosophila* and confirmed that these modifications are conserved in mice brains and human cells. Moreover, we established that these regulatory mechanisms were sufficient to modulate the expression levels of TDP-43 in both flies and human cells and to affect locomotor behaviors. Interestingly, a similar outcome was detected using chaetocin, a chemical compound capable of inhibiting Su(var)3-9-mediated H3K9 methylation (46). These data reinforce the idea that Su(var)3-9 plays a fundamental role in the epigenetic regulation of *TBPH* expression and identifies a compound capable of regulating the expression levels of this gene *in situ*, contributing to the development of potential pharmacological interventions against ALS or locomotor weakening in the future.

In connection with the mechanisms involved, it is unclear how aging might influence the activity of Su(var)3-9 or the methylation status of the TBPH/TDP-43 promoter considering

that the total amount of H3K9 methylation in the genome decreases with age (Supplementary Figure S2) (47). Intriguingly, we found that the presence of aging-related factors able to induce early senescence in cultured human cells, such as H_20_2 accumulation, leads to a reduction in TDP-43 protein expression mediated by the human-homolog gene *SUV39H1* (Figure 4C)**,** suggesting that the metabolic changes that precede and drive aging could modify/increase the function of this enzyme in specific regions or loci of the chromosome (48,49). In agreement with this idea, ChIP array analyses performed in *Drosophila* brains found the increased accumulation of the *Su(var)3-9* protein itself at the promoter region of *TBPH* during aging (50,51). In addition, we detected a slight but significant increase in *Su(var)3-9* expression in old flies (Supplementary Figure S3G), explaining how the accumulation of epigenetic modifications in this locus could happen over time (Figure 5). In any case, additional experiments are necessary to deepen our knowledge of the issues discussed above.

In conclusion, we have identified an unprecedented mechanism whereby Su(var)3-9 regulates the epigenetic status of the *TARDBP/TBPH* promoter and drives the progression of locomotor aging through the regulation of TDP-43/TBPH expression levels. This role of SUV39 seems to be evolutionarily conserved from *Drosophila* to vertebrates and may help to understand the interrelationships between human aging and neurodegenerative diseases.

Acknowledgments

We thank Dr. Wiesława Leśniak (Nencki Institute of Experimental Biology, Warsaw, Poland) for the SUV39H1 mutant cell lines. Prof. Gunter Reuter (Institute of Biology and Developmental Genetics, Halle, Germany), Dr. Marion Delattre (Department of Genetics and Evolution, University of Geneva, Geneva, Switzerland) for the *Su(var)3-9*^{6} and *G9a*^{RG5} fly stocks respectively, and Prof. Franco Pagani (ICGEB-Trieste) for sharing reagents. This work

253 was supported by AFM-Telethon (project 21025) and AriSLA (NOSRESCUEALS) awards
254 to L.C., and F.F.

255

256 **Author contributions**

257 M.M., G.R., L.C., and F.F. designed the experiments. M.M., G.R., C.P., and F.R. performed
258 the experiments and collected the data, and analyzed the results together with L.C., and F.F.
259 M.M., G.R., L.C., and F.F. wrote the manuscript.

260 **Competing Interests**

261 The authors declare no competing financial interests.

262 **Methods**

263 **Drosophila strains and rearing conditions**

264 Drosophila stocks were maintained on standard fly food (25 g/L corn flour, 5 g/L lyophilized
265 agar, 50 g/L sugar, 50 g/L fresh yeast, 2,5 mL/L Tegosept [10% in ethanol], and 2.5 mL/L
266 propionic acid) at 25 □C in a 12h light/dark cycle. All experiments were performed in the
267 same standard conditions, otherwise differently specified. The following fly strains were
268 purchased from the Bloomington Drosophila Stock Center (BDSC, Indiana University,
269 Bloomington, IN, USA): w^{1118} (BDSC #3605); *elav-GS* (BDSC #43642); *UAS-TBPH* (BDSC
270 #93601); *UAS-TBPH.F-L* (BDSC #93781); *UAS-mCD8-GFP* (BDSC #30002); *Su(var)3-*
271 9^{1}*/TM3* (BDSC #6209); *UAS-Su(var)3-9.lacI* (BDSC #93147); *UAS-hSUV39H1.HA* (BDSC
272 #84799); *elav-GAL4* (BDSC #77894); egg^{1473}*/SM1* (BDSC #30565). The *Su(var)3-*9^{6}/TM6B
273 allele was a kind gift of Gunter Reuter (52), the $G9a^{RG5}$ allele was a kind gift of Marion
274 Delattre (53).

275 **Climbing assays**

The locomotion activity was measured by quantification of geotactic response. Equal ratio of male and females of the desired ages will be transferred, without anesthesia, to a 15 ml conical tube, tapped to the bottom of the tube, and their subsequent climbing activity quantified as the percentage of flies reaching the top of the tube in 10s (54). The number of climbing events was scored for 5 consecutive times. Flies were assessed in batches of 15, at least three biological replicates were performed for each condition (13).

RU486-Induction protocol

The Gene Switch system was activated by adding the RU486 (Sigma-Aldrich #M8046) activator to the fly food. A stock solution of 50 mM RU486 in 95% ethanol was diluted to the final concentration of 0.5 mM in 2% sucrose and the solution was been added on the surface of standard cornmeal medium to feed adults.

Chaetocin treatment

Adult fly heads were separated from the bodies and incubated with 100 nM chaetocin (Sigma-Aldrich #C9492) or 100% Ethanol in Schneider's Medium supplemented with 10% FBS for 2 h at room temperature. Heads were then washed in PBS1x and collected for subsequent analysis.

Chromatin immunoprecipitation

Fly heads

Heads of frozen flies were separated by vortexing for 15 sec and isolated using 630 μm and 400 μm sieves. 400 – 600 fly heads were homogenized in homogenization buffer [350 mM sucrose, 15 mM HEPES pH 7.6, 10 mM KCl, 5 mM MgCl2, 0.5 mM EGTA, 0.1 mM EDTA, 0.1% Tween, with 1 mM DTT and Protease Inhibitor Cocktail (PIC, Roche) added immediately prior to use] at 4 °C. The homogenate was fixed using 1% formaldehyde for 10 min at RT and then quenched with glycine. The tissue debris was removed by filtration with 60 μm nylon net (Millipore). Nuclei were collected and washed with RIPA buffer at 4 °C

(150 mM NaCl, 25 mM HEPES pH 7.6, 1 mM EDTA, 1% Triton-X, 0.1% SDS, 0.1% DOC, with protease inhibitors added prior to use). The extract was sonicated 6 times with 2 min cycles (Branson Sonifier 250, output=50%). Sonicated samples were centrifuged for 10 min at 12,000 × *g*. Two hundred and fifty micrograms of chromatin DNA were subjected to a 1 h preclearing with 50 μl of a 50% protein G-Sepharose (GE healthcare) bead slurry containing 1% BSA. Before the Immunoprecipitation, 5% of the total extract was collected as INPUT. The precleared samples were then immunoprecipitated overnight with 5 μg of anti-H3K9me3 (Abcam ab8898) or anti-rabbit IgGs (Sigma, 15006) at 4 °C. The immune complexes were incubated for 4 h at 4 °C with 50 μl of fresh protein G-Sepharose beads. After immunopurification, beads were washed four times with RIPA and once with LiCl wash buffer (250 mM LiCl, 10 mM Tris-Hcl pH 8.0, 1 mM EDTA, 0.5% NP-40, protease inhibitors PIC (Roche). Beads were re-suspended in TE buffer and incubated ON at 65°C. Proteins were digested with Proteinase K (10 mg/ml) at 55 °C for 1 h. Immunoprecipitated DNA was purified using Phenol:Chlorophorm:Isoamyl alchol extraction. Immunoprecipitated DNA and 5% input DNA were analyzed by SYBR-Green real-time qPCR. The run was performed by using the Applied Biosystems (Waltham, MA) Quant-Studio 3 Real-Time PCR System 36 instrument. Primer Sequences described previously are reported in Table S1.

Mouse brain

Chromatin immunoprecipitation in brain of C57 mice at post-natal day 10 (PND 10) and PND 365 was performed using EpiQuik Tissue Chromatin Immunoprecipitation kit (Epigentek #P-2003) according to manufacturer's instructions. Briefly, 150 mg of frozen tissue were cut into small pieces (<1 mm^3) and cross-linked with 1% formaldehyde for 10 min at room temperature and then quenched in PBS 1X-Glycine 1.25M for 10 min at room temperature. The samples were homogenized using a Douncer homogenizer and centrifuged to pellet nuclei. After homogenization, lysis buffer was added to nuclei. Chromatin was

prepared and sonicated using a water bath Bioruptor (Diagenode; 30" ON/30" OFF, High power, 3 x 10 cycles) to a size range of 200 -1000 bp. To pre-cleared cell debris, sonicated chromatin was centrifuged at 12,000 x g at +4°C for 10 minutes. Chromatin was diluted and ChIP performed according to manufacturer's instructions using antibodies against H3K9me3 (ab8898, Abcam), histone H3 (ab1791, Abcam), IgG1 (G3A1, Cell Signalling) was used as negative control in the immunoprecipitation. Immunoprecipitated DNA was purified by phenol-chloroform extraction and in parallel 5 ul (5%) were taken to be used as input in the quantification analysis. qPCRs were performed using iQ SYBR Green in a CFX96 Real-Time PCR system (Bio-Rad). Primer sequences are reported in Table S1.

Human HaCaT cells

HaCaT cells were crosslinked with 1% formaldehyde fixing buffer (1% Formaldehyde; 5 mM Hepes pH8.0; 0.05 mM EGTA pH 8.0; 10 mM NaCl) at 37 °C for 10 minutes and then quenched with glycine, rinsed twice with cold phosphate-buffered saline, and then lysed and harvested in ChIP lysis buffer (50 mM Tris-HCl pH 8.1; 0.5% SDS; 10 mm EDTA;100 mM NaCl, 1mM PMSF, Proteinase inhibitor Roche) by centrifugation for 6 min at 2,000 × *g*. Cells were then resuspended in sonication buffer (50 mM Tris-HCl pH 8.1; 10 mm EDTA; 1% Triton-X; 0,1% deoxycholate_sodium; 100 mM NaCl, 1mM PMSF, Proteinase inhibitor Roche) and sonicated 6 times with 2 min cycles (Branson Sonifier 250, output=50%). Sonicated samples were centrifuged for 10 min at 12,000 × *g* and the supernatant were diluted 5-fold in sonication buffer. Two hundred and fifty micrograms of chromatin DNA were subjected to a 1 h preclearing with 50 μl of a 50% protein G-Sepharose (GE healthcare) bead slurry containing 1% BSA. Before the Immunoprecipitation, 5% of the total extract was collected as INPUT. The precleared samples were then immunoprecipitated overnight with 5 μg of anti-H3K9me3 (Abcam ab8898) at 4 °C. The immune complexes were then incubated for 4 h at 4 °C with 50 μl of fresh protein G-Sepharose beads. Following incubation, the

beads were collected by centrifugation for 1 min at 2,000 × *g* and washed consecutively for 3–5 min with 1 ml of each solution: low-salt wash buffer (0.1% SDS; 1% Triton X-100; 2 mM EDTA; 20 mM Tris pH 8.1; and 150 mM NaCl), high-salt wash buffer (0.1% SDS; 1% Triton X-100; 2 mM EDTA, 20 mM Tris pH 8.1; and 500 mM NaCl), LiCl wash buffer (250 mM LiCl; 1% NP-40, 1% deoxycholate sodium salt, 1 mM EDTA, and 10 mM Tris pH 8.1), and twice in Tris and EDTA buffers (10 mM Tris pH 8.1 and 1 mM EDTA). Immune complexes were then eluted with 120 μl of buffer containing 1% SDS and 100 mm $NaHCO_3$. Crosslinking was reversed by incubating the samples overnight at 65 °C. Proteins were digested with Proteinase K (10 mg/ml) at 55 °C for 1 h. Immunoprecipitated DNA was purified using Phenol:Chlorophorm:Isoamyl alcohol extraction. Immunoprecipitated DNA (1.5 µl) and 5% input DNA were analyzed by SYBR-Green real-time qPCR (as described in Antonucci et al 2014). The run was performed by using the Applied Biosystems (Waltham, MA) Quant-Studio 3 Real-Time PCR System 36 instrument. Primer Sequences described previously are reported in Table S1.

RNA extraction and quantitative PCR

Total mRNA was isolated from *Drosophila* adult heads by using Trizol reagent (15596026, Thermo Fisher Scientific) according to the manufacturer's instructions. RNA was reverse-transcribed (1 mg each experimental point) by using SensiFAST cDNA Synthesis Kit (BIO-65053, Bioline) and qPCR was performed as described (18) using SensiFast Sybr Lo-Rox Mix (BIO- 94020, Bioline). The run was performed by using the Applied Biosystems (Waltham, MA) Quant Studio 3 Real- Time PCR System 36 instrument. Primer Sequences are reported in Table S1.

Human HaCAT cells

The immortalized human epidermal keratinocyte (HaCaT) cell line was obtained from (19). The HaCaT cells were cultured in complete media, which comprised of Dulbecco's modified

Eagle's medium (DMEM) supplemented with 10% (v/v) heat-inactivated fetal bovine serum and 1% (v/v) penicillin-streptomycin at 37 °C in a humidified atmosphere of 5% CO_2/95% air.

H_2O_2 Treatment

HaCaT cells (10^5cells) were cultured on 35 mm cell culture dish for 24 h and treated with H_2O_2 at 200 µM/l for 2 h at 37 °C.

H_2O_2 was washed with PBS for terminating the treatment. Cells were kept on the incubation in normal medium for another 24 h. Cells were then harvested and assessed in western blot.

Western Blot

Fly extract

Protein extracts were derived from adult fly heads, lysed in sample buffer or Urea Buffer (150 mM NaCl, 10 mM Tris-HCl pH8, 0,5 mM EDTA, 10% glycerol, 5 mM EGTA, 50 mM NaF, 4 M urea, 5 mM DTT, Protease Inhibitor Cocktail (PIC) (Roche), fractionated by SDS-PAGE and transferred to nitrocellulose membrane. Primary antibodies were: anti-TBPH rabbit (1:1000; homemade (13); anti-Actin goat (1:1000; Santa Cruz, sc-1616); anti-Vibrator rabbit (1:5000; also named Giotto (55); anti-H3K9me2 mouse (1:400; Abcam ab1220), anti-H3K9me3 rabbit (1:1000; Abcam ab8898); anti-Tubulin mouse (1:5000; Sigma, T-5168); anti-HA HRP (1:1000; Santa Cruz sc7392); anti-Su(var)3-9 rat (1:50; (32). As a secondary antibody, we used the appropriate HRP-conjugated antibody (GE Healthcare) diluted 1:5000 in PBS-Tween 0.1%. Membranes were incubated 5 min with ECL substrate (#1705062 and #1705060, Bio-Rad) and the HRP-ECL reaction was revealed using the ChemiDoc™ XRS gel imaging system (Bio-Rad). Band intensity quantification was performed using the gel analyzer tool in Fiji/ImageJ software.

HaCAT extract

Cells were harvested and centrifuged at 5,000 rpm for 5 min at 4°C. The supernatant was

removed, Buffer WCE 2X (100 mM TrisHCl pH 6.8, 4% SDS, 200 mM DTT) was added to resuspend the cell pellet, boiled for 10 min and then added an equal volume of SDS-PAGE Sample Loading Buffer [2X] (100 mM TrisHCl pH 6.8, 4% SDS, 200 mM DTT, 20% glycerol, 0.004% bromphenol blue) to the mixture. Cell extracts were pelleted at 15,000 g in an Eppendorf centrifuge for 15 min at 4°C and the supernatants were analyzed by Western blotting according to (56), using the following antibodies, all diluted in TBS-T: anti-p-p53 (Ser 15; 1:1000, Santa Cell Signaling), anti-p53 (1:1000, Santa Cruz), anti-p-H2AX (Ser 139; 1:1000, Millipore), anti-SUV39H1 (44.1; 1:1000, Santa Cruz Biotechnology), anti-TDP-43 (1:5000, Proteintech), anti-H3k9me3 (1:1000, Abcam ab8898), anti-H3K9me2 (1:500, Abcam ab1220), anti-actin-HRP-conjugated (1:5000, Santa Cruz Biotechnology). These primary antibodies were detected using HRP conjugated anti-mouse and anti-rabbit IgGs and the ECL detection kit (all from GE Healthcare). Band intensities were quantified by densitometric analysis with Image Lab software (Bio-Rad).

All full length uncropped original western blots are available in the Supplementary Materials section.

Statistical analyses

Statistical analysis was performed using Prism six software (MacKiev). The Shapiro-Wilk test was used to assess the normal distribution of every group of different genotypes. Statistical differences for multiple comparisons were analyzed with the Kruskal-Wallis for non-parametric values or with one-way ANOVA for parametric values. The Dunn's or the Tukey's test was performed, respectively, as post hoc test to determine the significance between every single group. The Mann-Whitney U-test or the t-test were used for two groups' comparison of non-parametric or parametric values, respectively. A $p < 0.05$ was considered significant.

References

1. Fontana L, Partridge L, Longo VD. Dietary Restriction, Growth Factors and Aging: from yeast to humans. Science. 2010 Apr 16;328(5976):321–6.

2. DiLoreto R, Murphy CT. The cell biology of aging. Mol Biol Cell. 2015 Dec 15;26(25):4524–31.

3. da Silva PFL, Schumacher B. Principles of the Molecular and Cellular Mechanisms of Aging. J Invest Dermatol. 2021 Apr 1;141(4, Supplement):951–60.

4. Hussain R, Zubair H, Pursell S, Shahab M. Neurodegenerative Diseases: Regenerative Mechanisms and Novel Therapeutic Approaches. Brain Sci. 2018 Sep;8(9):177.

5. Di Giorgio ML, Esposito A, Maccallini P, Micheli E, Bavasso F, Gallotta I, et al. WDR79/TCAB1 plays a conserved role in the control of locomotion and ameliorates phenotypic defects in SMA models. Neurobiol Dis. 2017 Sep 1;105:42–50.

6. Hou Y, Dan X, Babbar M, Wei Y, Hasselbalch SG, Croteau DL, et al. Ageing as a risk factor for neurodegenerative disease. Nat Rev Neurol. 2019 Oct;15(10):565–81.

7. Stein D, Mizrahi A, Golova A, Saretzky A, Venzor AG, Slobodnik Z, et al. Aging and pathological aging signatures of the brain: through the focusing lens of SIRT6. Aging. 2021 Mar 9;13(5):6420–41.

8. Kane AE, Sinclair DA. Epigenetic changes during aging and their reprogramming potential. Crit Rev Biochem Mol Biol. 2019 Feb;54(1):61–83.

9. Wang K, Liu H, Hu Q, Wang L, Liu J, Zheng Z, et al. Epigenetic regulation of aging: implications for interventions of aging and diseases. Signal Transduct Target Ther. 2022 Nov 7;7(1):1–22.

10. Arai T, Hasegawa M, Akiyama H, Ikeda K, Nonaka T, Mori H, et al. TDP-43 is a component of ubiquitin-positive tau-negative inclusions in frontotemporal lobar degeneration and amyotrophic lateral sclerosis. Biochem Biophys Res Commun. 2006 Dec 22;351(3):602–11.

11. Neumann M, Sampathu DM, Kwong LK, Truax AC, Micsenyi MC, Chou TT, et al. Ubiquitinated TDP-43 in frontotemporal lobar degeneration and amyotrophic lateral sclerosis. Science. 2006 Oct 6;314(5796):130–3.

12. Sreedharan J, Blair IP, Tripathi VB, Hu X, Vance C, Rogelj B, et al. TDP-43 mutations in familial and sporadic amyotrophic lateral sclerosis. Science. 2008 Mar 21;319(5870):1668–72.

13. Feiguin F, Godena VK, Romano G, D'Ambrogio A, Klima R, Baralle FE. Depletion of TDP-43 affects Drosophila motoneurons terminal synapsis and locomotive behavior. FEBS Lett. 2009 May 19;583(10):1586–92.

14. Romano G, Klima R, Buratti E, Verstreken P, Baralle FE, Feiguin F. Chronological requirements of TDP-43 function in synaptic organization and locomotive control. Neurobiol Dis. 2014 Aug 1;

15. Cragnaz L, Klima R, De Conti L, Romano G, Feiguin F, Buratti E, et al. An age-related reduction of brain TBPH/TDP-43 levels precedes the onset of locomotion defects in a Drosophila ALS model. Neuroscience. 2015 Dec 17;311:415–21.

16. Pacetti M, De Conti L, Marasco LE, Romano M, Rashid MM, Nubiè M, et al. Physiological tissue-specific and age-related reduction of mouse TDP-43 levels is regulated by epigenetic modifications. Dis Model Mech. 2022 01;15(4).

17. Strah N, Romano G, Introna C, Klima R, Marzullo M, Ciapponi L, et al. TDP-43 promotes the formation of neuromuscular synapses through the regulation of Disc-large expression in Drosophila skeletal muscles. BMC Biol. 2020 Mar 26;18(1):34.

18. Romano G, Holodkov N, Klima R, Grilli F, Guarnaccia C, Nizzardo M, et al. Downregulation of glutamic acid decarboxylase in Drosophila TDP-43-null brains provokes paralysis by affecting the organization of the neuromuscular synapses. Sci Rep. 2018 Jan 29;8(1):1809.

19. Romano G, Klima R, Feiguin F. TDP-43 prevents retrotransposon activation in the Drosophila motor system through regulation of Dicer-2 activity. BMC Biol. 2020 Jul 3;18(1):82.

20. Romano G, Appocher C, Scorzeto M, Klima R, Baralle FE, Megighian A, et al. Glial TDP-43 regulates axon wrapping, GluRIIA clustering and fly motility by autonomous and non-autonomous mechanisms. Hum Mol Genet. 2015 Nov 1;24(21):6134–45.

21. Langellotti S, Romano V, Romano G, Klima R, Feiguin F, Cragnaz L, et al. A novel fly model of TDP-43 proteinopathies: N-terminus sequences combined with the Q/N domain induce protein functional loss and locomotion defects. Dis Model Mech. 2016 Apr 21;

22. Rhodenizer D, Martin I, Bhandari P, Pletcher SD, Grotewiel M. Genetic and environmental factors impact age-related impairment of negative geotaxis in Drosophila by altering age-dependent climbing speed. Exp Gerontol. 2008 Aug;43(8):739–48.

23. Jones MA, Grotewiel M. Drosophila as a model for age-related impairment in locomotor and other behaviors. Exp Gerontol. 2011 May;46(5):320–5.

24. Osterwalder T, Yoon KS, White BH, Keshishian H. A conditional tissue-specific transgene expression system using inducible GAL4. Proc Natl Acad Sci U S A. 2001 Oct 23;98(22):12596–601.

25. Roman G, Endo K, Zong L, Davis RL. P[Switch], a system for spatial and temporal control of gene expression in Drosophila melanogaster. Proc Natl Acad Sci U S A. 2001 Oct 23;98(22):12602–7.

26. Godena VK, Romano G, Romano M, Appocher C, Klima R, Buratti E, et al. TDP-43 Regulates Drosophila Neuromuscular Junctions Growth by Modulating Futsch/MAP1B Levels and Synaptic Microtubules Organization. PLOS ONE. 2011 Mar 11;6(3):e17808.

27. Bannister AJ, Kouzarides T. Regulation of chromatin by histone modifications. Cell Res. 2011 Mar;21(3):381–95.

28. Waddington CH. The Epigenotype. Int J Epidemiol. 2012 Feb 1;41(1):10–3.

29. Tschiersch B, Hofmann A, Krauss V, Dorn R, Korge G, Reuter G. The protein encoded by the Drosophila position-effect variegation suppressor gene Su(var)3-9 combines domains of antagonistic regulators of homeotic gene complexes. EMBO J. 1994 Aug 15;13(16):3822–31.

30. Padeken J, Methot SP, Gasser SM. Establishment of H3K9-methylated heterochromatin and its functions in tissue differentiation and maintenance. Nat Rev Mol Cell Biol. 2022 Sep;23(9):623–40.

31. McCauley BS, Dang W. Histone methylation and aging: Lessons learned from model systems. Biochim Biophys Acta BBA - Gene Regul Mech. 2014 Dec 1;1839(12):1454–62.

32. Schotta G, Ebert A, Krauss V, Fischer A, Hoffmann J, Rea S, et al. Central role of Drosophila SU(VAR)3–9 in histone H3-K9 methylation and heterochromatic gene silencing. EMBO J. 2002 Mar 1;21(5):1121–31.

33. Kwiatkowski TJ Jr, Bosco DA, Leclerc AL, Tamrazian E, Vanderburg CR, Russ C, et al. Mutations in the FUS/TLS gene on chromosome 16 cause familial amyotrophic lateral sclerosis. Science. 2009 Feb 27;323(5918):1205–8.

34. Sobiak B, Leśniak W. Effect of SUV39H1 Histone Methyltransferase Knockout on Expression of Differentiation-Associated Genes in HaCaT Keratinocytes. Cells. 2020 Dec;9(12):2628.

35. Tripathi M, Yen PM, Singh BK. Protocol to Generate Senescent Cells from the Mouse Hepatic Cell Line AML12 to Study Hepatic Aging. STAR Protoc. 2020 Sep 18;1(2):100064.

36. Ngian ZK, Lin WQ, Ong CT. NELF-A controls Drosophila healthspan by regulating heat-shock protein-mediated cellular protection and heterochromatin maintenance. Aging Cell. 2021 May;20(5):e13348.

37. Stead ER, Bjedov I. Balancing DNA repair to prevent ageing and cancer. Exp Cell Res. 2021 Aug 15;405(2):112679.

38. Liu Y, Atkinson RAK, Fernandez-Martos CM, Kirkcaldie MTK, Cui H, Vickers JC, et al. Changes in TDP-43 expression in development, aging, and in the neurofilament light protein knockout mouse. Neurobiol Aging. 2015 Feb 1;36(2):1151–9.

39. Scotter EL, Chen HJ, Shaw CE. TDP-43 Proteinopathy and ALS: Insights into Disease Mechanisms and Therapeutic Targets. Neurotherapeutics. 2015 Apr 1;12(2):352–63.

40. Prasad A, Bharathi V, Sivalingam V, Girdhar A, Patel BK. Molecular Mechanisms of TDP-43 Misfolding and Pathology in Amyotrophic Lateral Sclerosis. Front Mol Neurosci [Internet]. 2019 [cited 2021 May 27];12. Available from: https://www.frontiersin.org/articles/10.3389/fnmol.2019.00025/full

41. Boer EMJ de, Orie VK, Williams T, Baker MR, Oliveira HMD, Polvikoski T, et al. TDP-43 proteinopathies: a new wave of neurodegenerative diseases. J Neurol Neurosurg Psychiatry. 2021 Jan 1;92(1):86–95.

42. Van Deerlin VM, Leverenz JB, Bekris LM, Bird TD, Yuan W, Elman LB, et al. TARDBP mutations in amyotrophic lateral sclerosis with TDP-43 neuropathology: a genetic and histopathological analysis. Lancet Neurol. 2008 May;7(5):409–16.

43. Neumann M, Tolnay M, Mackenzie IRA. The molecular basis of frontotemporal dementia. Expert Rev Mol Med. 2009;11:e23.

44. Iguchi Y, Katsuno M, Niwa J ichi, Takagi S, Ishigaki S, Ikenaka K, et al. Loss of TDP-43 causes age-dependent progressive motor neuron degeneration. Brain. 2013 May 1;136(5):1371–82.

555 45. Yang C, Wang H, Qiao T, Yang B, Aliaga L, Qiu L, et al. Partial loss of TDP-43 function
556 causes phenotypes of amyotrophic lateral sclerosis. Proc Natl Acad Sci. 2014 Mar
557 25;111(12):E1121–9.

558 46. Greiner D, Bonaldi T, Eskeland R, Roemer E, Imhof A. Identification of a specific
559 inhibitor of the histone methyltransferase SU(VAR)3-9. Nat Chem Biol. 2005
560 Aug;1(3):143–5.

561 47. Wood JG, Jones BC, Jiang N, Chang C, Hosier S, Wickremesinghe P, et al. Chromatin-
562 modifying genetic interventions suppress age-associated transposable element activation
563 and extend life span in *Drosophila*. Proc Natl Acad Sci. 2016 Oct 4;113(40):11277–82.

564 48. Luquin N, Yu B, Saunderson RB, Trent RJ, Pamphlett R. Genetic variants in the
565 promoter of TARDBP in sporadic amyotrophic lateral sclerosis. Neuromuscul Disord.
566 2009 Oct 1;19(10):696–700.

567 49. Peng JC, Karpen GH. H3K9 methylation and RNA interference regulate nucleolar
568 organization and repeated DNA stability. Nat Cell Biol. 2007 Jan;9(1):25–35.

569 50. Riddle NC, Minoda A, Kharchenko PV, Alekseyenko AA, Schwartz YB, Tolstorukov
570 MY, et al. Plasticity in patterns of histone modifications and chromosomal proteins in
571 Drosophila heterochromatin. Genome Res [Internet]. 2010 Dec 22 [cited 2023 Mar 5];
572 Available from: https://genome.cshlp.org/content/early/2011/01/10/gr.110098.110

573 51. Ho JWK, Jung YL, Liu T, Alver BH, Lee S, Ikegami K, et al. Comparative analysis of
574 metazoan chromatin organization. Nature. 2014 Aug;512(7515):449–52.

52. Schotta G, Lachner M, Sarma K, Ebert A, Sengupta R, Reuter G, et al. A silencing pathway to induce H3-K9 and H4-K20 trimethylation at constitutive heterochromatin. Genes Dev. 2004 Jun 1;18(11):1251–62.

53. Seum C, Reo E, Peng H, Iii FJR, Spierer P, Bontron S. Drosophila SETDB1 Is Required for Chromosome 4 Silencing. PLOS Genet. 2007 May 11;3(5):e76.

54. Madabattula ST, Strautman JC, Bysice AM, O'Sullivan JA, Androschuk A, Rosenfelt C, et al. Quantitative Analysis of Climbing Defects in a Drosophila Model of Neurodegenerative Disorders. JoVE J Vis Exp. 2015 Jun 13;(100):e52741.

55. Porrazzo A, Cipressa F, De Gregorio A, De Pittà C, Sales G, Ciapponi L, et al. Low dose rate γ-irradiation protects fruit fly chromosomes from double strand breaks and telomere fusions by reducing the esi-RNA biogenesis factor Loquacious. Commun Biol. 2022 Sep 3;5(1):905.

56. Coni S, Falconio FA, Marzullo M, Munafò M, Zuliani B, Mosti F, et al. Translational control of polyamine metabolism by CNBP is required for Drosophila locomotor function. Ramaswami M, VijayRaghavan K, Ramaswami M, editors. eLife. 2021 Sep 14;10:e69269.

Figure Legends

Figure 1. TBPH prevents locomotory senescence in Drosophila

(**A**) Schematic representation of the *elav*-Gene Switch induction protocol with RU486 (in green). The drug was added to fly food at day 18 until day 21, then the flies were transferred to standard food. (**B**) Western blot showing the TBPH levels in protein extracts from fly heads of the reported genotypes 1, 2 and 3 at day 18, day 21 in drug (RU486) or vehicle-only treated. Membranes were probed with anti-TBPH and anti-tubulin antibodies. Lane 1= UAS-GFPmCD8/+;*elav*GS/+; lane 2= +/+;*elav*GS/UAS-TBPH$^{F/L}$; lane 3= UAS-TBPH/+;*elav*GS/+;. Numbers below represent band quantification normalized on internal loading (tubulin). Average of two experiments. (**C**) Climbing assay in adult flies of the reported genotypes (+/+;*elav*GS/UAS-TBPH$^{F/L}$; and UAS-TBPH/+;*elav*GS/+), without (pink and blue, respectively) or with RU486 (orange and green, respectively) induction at different days post eclosion (7, 14, 18 and 21 dpe). Each point represents the percentage of flies able to reach the top of a 50 ml tube in 10 seconds after being tapped to the bottom. n≥ 100 animals for each genotype, in at least three technical replicates. ns, not significant; ** $p<0.01$ calculated by one-way ANOVA. Error bars represent SEM.

Figure 2. Levels of H3K9me3 at *TBPH/TARDBP* promoter increase with age

(**A**) qRT-PCR analysis on the *TBPH* promoter or on a control heterochromatic region (*rolled*), immunoprecipitated either with an anti-H3K9me3 antibody or with a control IgG antiserum in chromatin extracts from 3- or 20-days post eclosion (dpe) fly heads. The DNA enrichment is shown as a percentage of input DNA and normalized on the *GADPH* gene used as control. Note the significant increase (~2 fold) of *TBPH* promoter in 21 dpe flies compared with 3 dpe. No significant changes were observed in the control gene (*rolled*). Error bars represent SEM of three independent experiments (n = 3; pull of 300 heads), 3 biological

replicates and 3 technical replicates); $^{**}p = 0.0019$, ns, not significant; Mann-Whitney t-test. (**B**) qRT-PCR analysis on the *TARDBP* promoter or on the *GADPH-5'UTR* gene used as control, immunoprecipitated either with an anti-H3K9me3 antibody or with a control IgG antiserum in the brain of C57 mice at post-natal day 10 (PND 10) or PND 365. The DNA enrichment is shown as a percentage of input DNA and normalized on the total H3. Note the significant increase (~20 fold) of *m-TARDBP* promoter in PND 365 mice compared with PND 10. No significant changes were observed in the control gene (*m-GADPH*). Error bars represent SEM of three independent experiments (n = 6 mice per group, 3 biological replicates); *** p<0.001, ns, not significant; Mann-Whitney t-test.

Figure 3. Loss of Su(var)3-9 rescues TBPH ageing-dependent decrease and associated reduced climbing abilities

(**A**) Climbing assay performed in *Su(var)3-9* mutant flies (*Su(var)3-9^{6}/Su(var)3-9^{1};* red curve) or in control flies (*w^{1118};* blue curve), at different days post eclosion (3, 10, 20, 30 or 40 dpe). Each square represents the percentage of flies able to reach the top of a 50 ml tube in 10 seconds after being tapped to the bottom. n≥ 30 animals for each genotype, in at least five technical replicates. ns, not significative; *** p<0.001; ****p<0.0001 with one-way ANOVA. Error bars represent SEM. (**B**) qRT-PCR showing *TBPH* mRNA levels in *Su(var)3-9* mutants [*Su(var)3-9^{6}/Su(var)3-9^{1};* red] compared to controls (*w^{1118}*; blue) in RNAs from young (3dpe; full circles) or old (20 dpe; empty-dotted circles) flies heads extracts. Error bars represent SEM of three independent experiments (*n* = 3; pull of 50 heads), 3 biological replicates and 3 technical replicates). ** p<0.01; ****p<0.0001 with one-way ANOVA. (**C**) Western Blot showing the TBPH protein levels in *Su(var)3-9* mutants [*Su(var)3-9^{6}/Su(var)3-9^{1}*] compared to controls (*w^{1118}*) in fly head extracts at different days post eclosion (3, 20, 30 or 40 dpe). Numbers below represent band quantification (the average of four experiments) normalized on internal loading (Vibrator, Vib). (**D**) qRT-PCR

analysis on both the *TBPH* promoter and its coding sequence compared to a control heterochromatic region (*rolled*), immunoprecipitated either with an anti-H3K9me3 antibody or with a control IgG antisera in chromatin extracts from young (3 dpe) or old (20 dpe) *Su(var)3-9* mutants [$Su(var)3\text{-}9^{6}/Su(var)3\text{-}9^{1}$] or controls ($w^{1118}$). The DNA enrichment is shown as a percentage of input DNA and normalized on the *GAPDH* gene used as control. Error bars represent SEM of three independent experiments (n =3; pull of 300 heads, 3 biological replicates and 3 technical replicates). ** p<0.01; ****p<0.0001 with one-way ANOVA. (**E**) Climbing assay performed in adult flies overexpressing UAS-*Su(var)3-9 (*gray curve*),* or *UAS-hSuv39h1-HA (orange curve)* under the control of the *elav-GAL4* driver or in control flies expressing a *UAS-GFP* construct (blue curve), at different days post eclosion (3, 7, or 12 dpe), at 29°C. Each dot represents the percentage of flies that reach the top of a 50 ml tube in 10 seconds after being tapped to the bottom. n≥ 30 animals for each genotype, at least 5 technical replicates. ** p<0.01 *** p<0.001; ****p<0.0001 calculated by one-way ANOVA. (**F**) Western Blot showing the TBPH protein levels in heads extracts of flies overexpressing the *UAS-Su(var)3-9* or the *UAS-hSuv39h1-HA* or *UAS-GFP* under the control of the *elav-GAL4* driver at 3 days post eclosion. Numbers below represent band quantification normalized on internal loading (Vibrator, Vib).

Figure 4. SUV39H1 depletion in human cells correlates with reduced levels of H3K9me3 at T*ARDBP* promoter and with a corresponding increase in TDP-43 protein

(**A**) Western Blot showing the SUV39H1 and TDP-43 protein levels in extracts from WT or SUV39H1 KO cells. Numbers below represent band quantification normalized on internal loading control (actin; average of 6 experiments). (**B**) qRT-PCR analysis on the *hTARDBP* promoter immunoprecipitated with an anti-H3K9me3 in chromatin extracts from WT or SUV39H1 KO cells. Enrichment is shown as a percentage of input DNA and normalized on the *GADPH* gene used as control. Error bars represent SEM of three independent experiments

(*n* = 3, 3 biological replicates). (**C**) Western blots showing the expression levels of TDP-43 in wild type (WT) or *SUV39H1 KO* HaCaT Keratinocytes after (+) or not (-) treatment with H_2O_2 (200mM) for 2 ours (2h). H_2O_2 treatment reduces TDP-43 levels in WT but not in SUV39H1-KO cells. Numbers below represent band quantification normalized on internal loading control (actin; average of 3 biological repetitions).

Figure 5. Schematic representation of the mechanism of action of Suv39 at *TARDBP/TBPH* promoter region during aging. SUV39 activity at the *TARDBP/TBPH* promoter region is increased in elderly individuals. This effect results in increased methylation of H3K9 leading to reduced levels of TDP-43 expression and diminished locomotor capabilities.

Figure 1

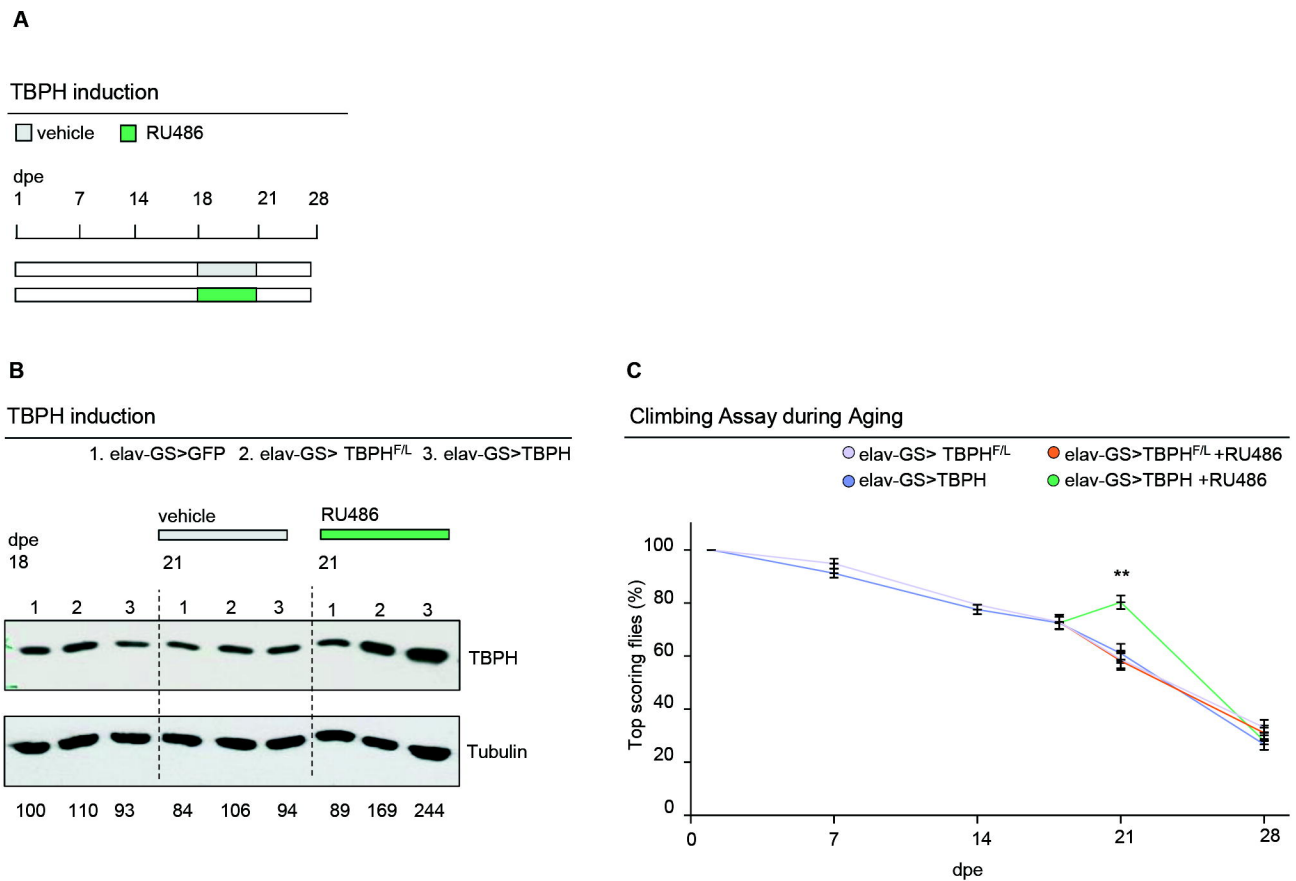
A
TBPH induction
vehicle
RU486
dpe
1
7
14
18
21
28
B
TBPH induction
1. elav-GS>GFP
2. elav-GS> TBPH$^{F/L}$
3. elav-GS>TBPH
vehicle
RU486
dpe
18
21
21
1 2 3 1 2 3 1 2 3
TBPH
Tubulin
100 110 93 84 106 94 89 169 244
C
Climbing Assay during Aging
elav-GS> TBPH$^{F/L}$
elav-GS>TBPH
elav-GS>TBPH$^{F/L}$ +RU486
elav-GS>TBPH +RU486
Top scoring flies (%)
100
80
60
40
20
0
**
0
7
14
21
28
dpe

Figure 2

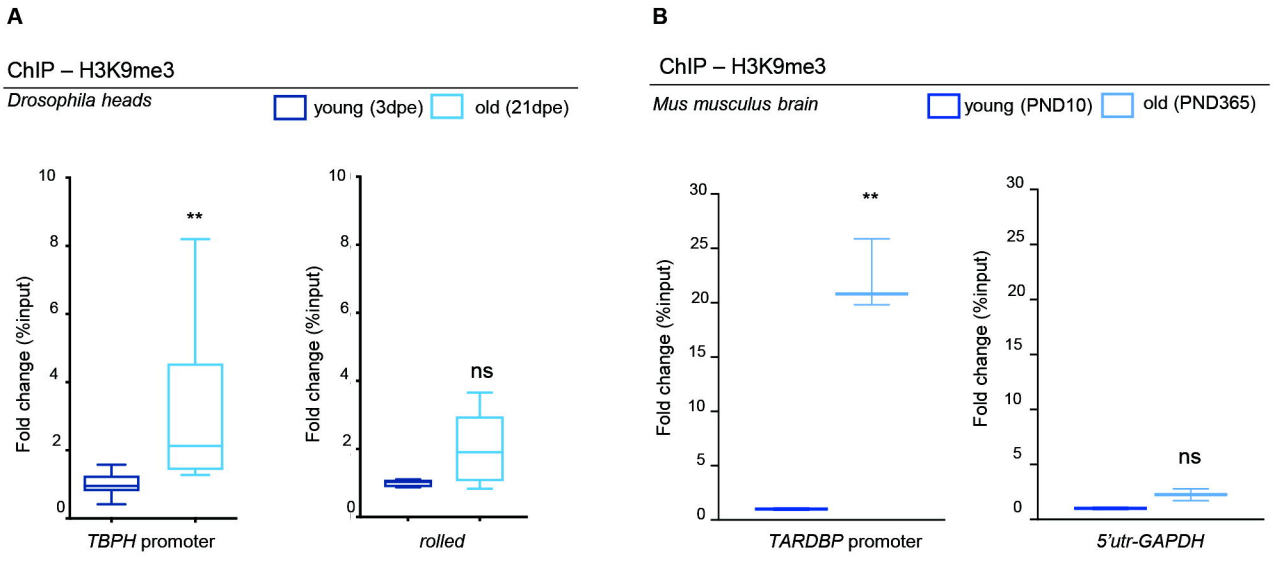
A
ChIP – H3K9me3
Drosophila heads
young (3dpe)
old (21dpe)
Fold change (%input)
**
ns
TBPH promoter
rolled
B
ChIP – H3K9me3
Mus musculus brain
young (PND10)
old (PND365)
Fold change (%input)
**
ns
TARDBP promoter
5'utr-GAPDH

Figure 3

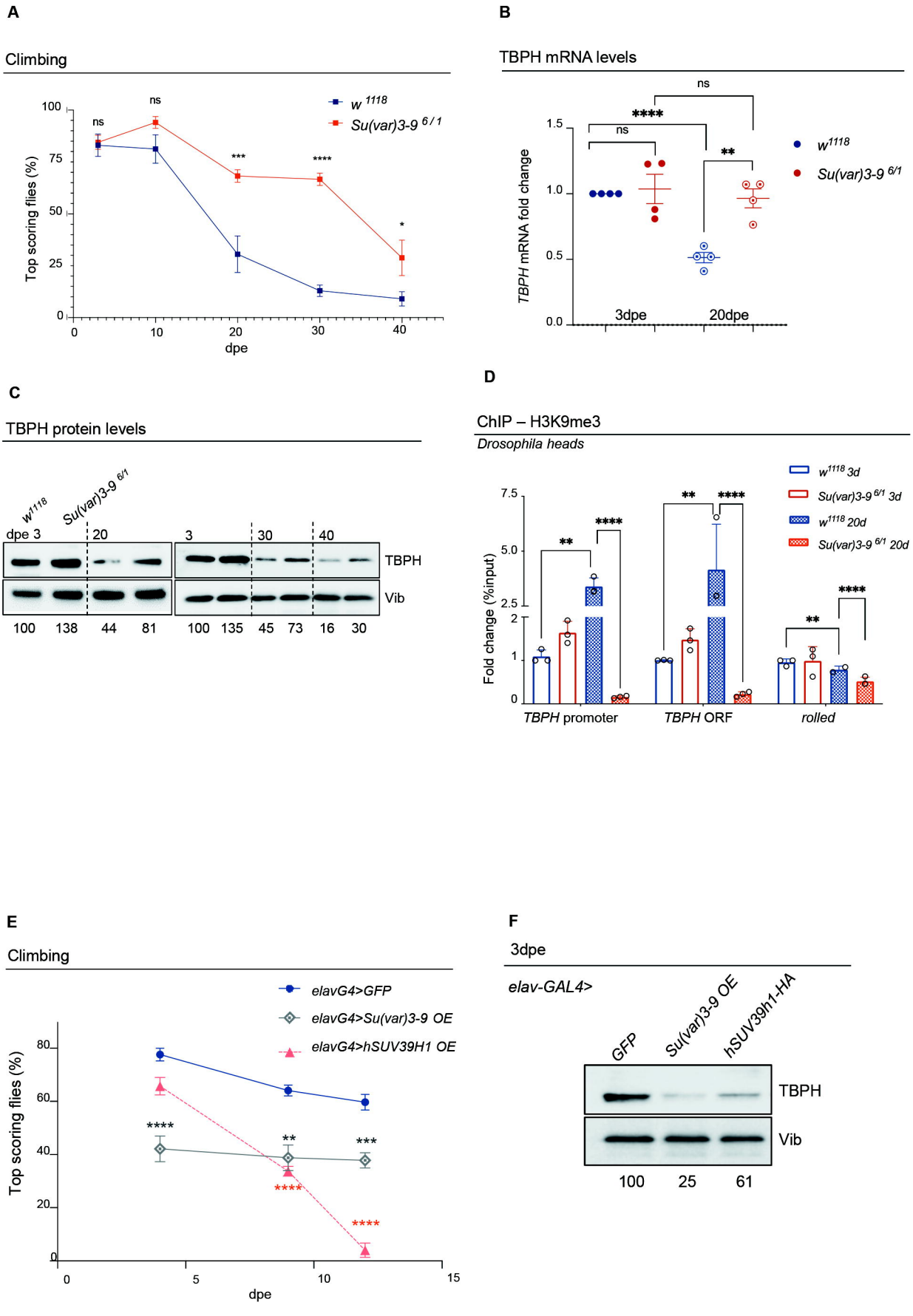
A
Climbing
Top scoring flies (%)
dpe
w 1118
Su(var)3-9 6/1
ns
***
****
*
B
TBPH mRNA levels
TBPH mRNA fold change
3dpe
20dpe
w1118
Su(var)3-9 6/1
****
**
C
TBPH protein levels
dpe 3
TBPH
Vib
100 138 44 81 100 135 45 73 16 30
D
ChIP – H3K9me3
Drosophila heads
Fold change (%input)
w1118 3d
Su(var)3-9 6/1 3d
w1118 20d
Su(var)3-9 6/1 20d
TBPH promoter
TBPH ORF
rolled
E
Climbing
Top scoring flies (%)
dpe
elavG4>GFP
elavG4>Su(var)3-9 OE
elavG4>hSUV39H1 OE
F
3dpe
elav-GAL4>
GFP
Su(var)3-9 OE
hSUV39h1-HA
TBPH
Vib
100 25 61

Figure 4

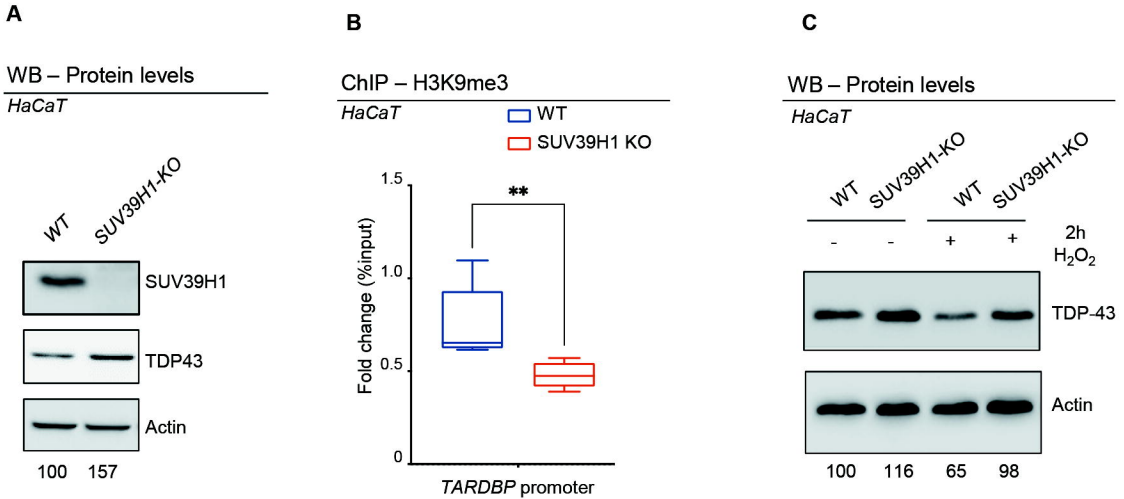
A
WB – Protein levels
HaCaT
WT
SUV39H1-KO
SUV39H1
TDP43
Actin
100
157
B
ChIP – H3K9me3
HaCaT
WT
SUV39H1 KO
**
Fold change (%input)
1.5
1.0
0.5
0
TARDBP promoter
C
WB – Protein levels
HaCaT
WT
SUV39H1-KO
WT
SUV39H1-KO
-
-
+
+
2h
H2O2
TDP-43
Actin
100
116
65
98

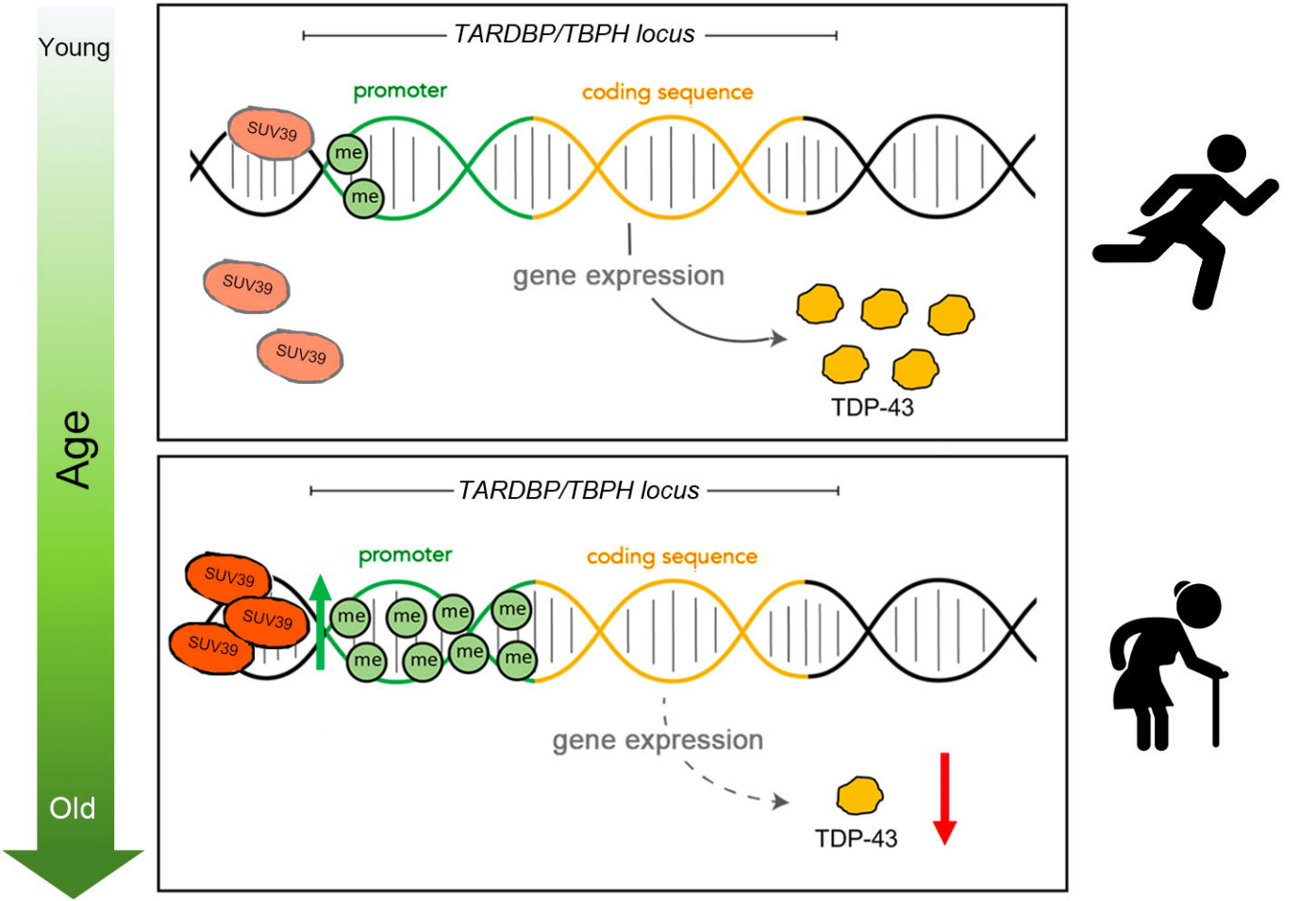
Young
Age
Old
TARDBP/TBPH locus
promoter
coding sequence
SUV39
me
gene expression
TDP-43
TARDBP/TBPH locus
promoter
coding sequence
SUV39
me
gene expression
TDP-43